Phase diffusion pattern in quantum nondemolition systems

Subhashish Banerjee*

Raman Research Institute, Bangalore - 560 080, India

Joyee Ghosh and R. Ghosh

School of Physical Sciences, Jawaharlal Nehru University, New Delhi - 110 067, India

(Dated: 27 March 2007)

We quantitatively analyze the dynamics of the quantum phase distribution associated with the reduced density matrix of a system, as the system evolves under the influence of its environment with an energy-preserving quantum nondemolition (QND) type of coupling. We take the system to be either an oscillator (harmonic or anharmonic) or a two-level atom (or equivalently, a spin-1/2 system), and model the environment as a bath of harmonic oscillators, initially in a general squeezed thermal state. The impact of the different environmental parameters is explicitly brought out as the system starts out in various initial states. The results are applicable to a variety of physical systems now studied experimentally with QND measurements.

PACS numbers: 03.65.Yz, 03.65.Vf, 42.50.Ct

I. INTRODUCTION

The theory of open quantum systems addresses the problems of damping and dephasing in quantum systems by its assertion that all real systems of interest are in fact 'open' systems, each surrounded by its environment. Quantum optics provided one of the first testing grounds for the application of the formalism of open quantum systems [1]. Application of open system ideas to other areas of physics was intensified by the works of Caldeira and Leggett [2], and Zurek [3] among others. Most such studies are based on a model describing quantum Brownian motion of a simple harmonic oscillator in a harmonic oscillator environment. In such a model studied by Caldeira and Leggett [2], the coordinate of the particle was coupled linearly to the harmonic oscillator reservoir, and it was also assumed that the system and the environment were initially separable. The treatment of the quantum Brownian motion has since been generalized to the physically reasonable initial condition of a mixed state of the system and its environment by Hakim and Ambegaokar [4], Smith and Caldeira [5], Grabert, Schramm and Ingold [6], and by us for the case of a system in a Stern-Gerlach potential [7], and also for the quantum Brownian motion with nonlinear system-environment couplings [8].

The recent upsurge of interest in the problem of open quantum systems is because of the spectacular progress in manipulation of quantum states of matter (atoms, or bosonic or fermionic gases or molecules), encoding, transmission and processing of quantum information, for all of which understanding and control of the environmental impact are essential. For such open quantum systems, there exists an important class of energy-preserving measurements in which dephasing occurs without damping of the system. This may be achieved with a particular type of coupling between the system and its environment, viz., when the Hamiltonian H_S of the system commutes with the Hamiltonian H_{SR} describing the system-reservoir interaction, i.e., H_{SR} is a constant of motion generated by H_S [9, 10, 11]. This condition describes a particular type of quantum nondemolition (QND) measurement scheme.

In general, a class of observables that may be measured repeatedly with arbitrary precision, with the influence of the measurement apparatus on the system being confined strictly to the conjugate observables, is called QND or back-action evasive observables [12, 13]. Such a measurement scheme was originally introduced in the context of the detection of gravitational waves [14, 15, 16, 17, 18, 19, 20]. The experimental progress on QND measurements has been summarized in the review [21] and the dynamics of decoherence in continuous atom-optical QND measurements studied in [22]. In addition to its relevance in ultrasensitive measurements, a QND scheme provides a way to prepare quantum mechanical states which may otherwise be difficult to create, such as Fock states with a specific number of particles. It has been shown that the accuracy of atomic interferometry can be improved by using QND measurements of the atomic populations at the inputs to the interferometer [23]. QND systems have also been proposed for engineering quantum dynamical evolution of a system with the help of a quantum meter [24]. We have recently studied such QND open system Hamiltonians for two different models of the environment describable as baths of either oscillators

---

*Electronic address: subhashishb@rri.res.in

or spins, and found an interesting connection between the energy-preserving QND Hamiltonians and the phase space area-preserving canonical transformations [25].

As stated above, in the context of energy-preserving QND systems, the only effect of the environment on the system is dephasing and it is a natural question to ask about the pattern of diffusion of 'phases' in such a situation. Such a question is particularly relevant in the context of a number of practical phase measurement schemes [23, 26].

What is the precise meaning of the quantum mechanical phase? The quantum description of phases [27] has a long history [28, 29, 30, 31, 32]. Pegg and Barnett [31], following Dirac [28], carried out a polar decomposition of the annihilation operator and defined a hermitian phase operator in a finite-dimensional Hilbert space. In their scheme, the expectation value of a function of the phase operator is first carried out in a finite-dimensional Hilbert space, and then the dimension is taken to the limit of infinity. However, it is not possible to interpret this expectation value as that of a function of a hermitian phase operator in an infinite-dimensional Hilbert space [33, 34]. To circumvent this problem, the concept of phase distribution for the quantum phase has been introduced [33, 35]. In this scheme, one associates a phase distribution to a given state such that the average of a function of the phase operator in the state, computed with the phase distribution, reproduces the results of Pegg and Barnett.

In this paper we address the problem of quantum phase diffusion and study the dynamics of the quantum phase distribution associated with the reduced density matrix of the system for a number of situations of practical importance, as the system evolves under the influence of its environment with an energy-preserving QND coupling. One may take the system to be either an oscillator (harmonic or anharmonic) or a two-level atom (or equivalently, a spin-1/2 system). The phase distributions associated with the quantum state for the two cases are defined. The environment is modeled as a bath of harmonic oscillators, and the impact of the environmental parameters is quantified for different initial states of the system.

The plan of the paper is as follows. In Section II, we briefly discuss a generic energy-preserving QND system in the context of open systems [36]. The bath is taken to be initially in a squeezed thermal state, from which the common thermal bath results may be easily extracted by setting the squeezing parameters to zero. In Section III, we define the phase distribution for an oscillator system, following Agarwal *et al.* [35]. In Section IIIA in particular, we consider a harmonic oscillator system in QND interaction with its environment [26]. We study two different initial conditions, of the system starting (1) in a coherent state and (2) in a squeezed coherent state. In Section IIIB, we study the case where the system is an anharmonic oscillator, which could arise, for example, from the interaction of a single mode of the quantized electromagnetic field with a Kerr medium [37, 38]. This Hamiltonian can be expressed in terms of the generators of the group SU(1,1). Using the positive discrete series representation of this group, we construct its phase distribution and study it for two different situations: (1) when the system is initially in a Kerr state, and (2) when it is initially in a squeezed Kerr state [37]. In Section IV we consider the phase distribution for a two-level atom, extensively used as a model system in quantum computation [39, 40, 41]. Following the phase distribution of angular momentum systems introduced by Agarwal and Singh [42], we construct and study the phase distribution of the system for three different initial conditions of the system, starting (1) in a Wigner-Dicke state [43], which is the atomic analogue of the standard Fock state [44], (2) in an atomic coherent state, which is the atomic analogue of the Glauber coherent state [44], and (3) in an atomic squeezed state [42, 45]. In Section V we present our conclusions.

II. GENERIC QND OPEN SYSTEMS

We consider the following Hamiltonian describing the interaction of a system with its environment, modeled as a reservoir of harmonic oscillators, via a QND type of coupling [36]:

$$
\begin{aligned}
H &= H_S + H_R + H_{SR} \\
&= H_S + \sum_k \hbar \omega_k b_k^\dagger b_k + H_S \sum_k g_k (b_k + b_k^\dagger) + H_S^2 \sum_k \frac{g_k^2}{\hbar \omega_k}.
\end{aligned}
\tag{1}
$$

Here H_S, H_R and H_{SR} stand for the Hamiltonians of the system, reservoir and system-reservoir interaction, respectively. H_S is a generic system Hamiltonian which we will specify in the subsequent sections to model different physical situations. $b_k^\dagger$, b_k denote the creation and annihilation operators for the reservoir oscillator of frequency ω_k, g_k stands for the coupling constant (assumed real) for the interaction of the oscillator field with the system. The last term on the right-hand side of Eq. (1) is a renormalization inducing 'counter term'. Since $[H_S, H_{SR}] = 0$, the Hamiltonian (1) is of QND type. The system plus reservoir composite is closed obeying a unitary evolution given by

$$
\rho(t) = e^{-\frac{i}{\hbar} H t} \rho(0) e^{\frac{i}{\hbar} H t},
\tag{2}
$$

where

$$
\rho(0) = \rho^s(0) \rho_R(0),
\tag{3}
$$

i.e., we assume separable initial conditions. The reservoir is assumed to be initially in a squeezed thermal state, i.e., it is a squeezed thermal bath, with an initial density matrix $\rho_R(0)$ given by

$$\hat{\rho}_R(0) = \hat{S}(r,\Phi)\hat{\rho}_{th}\hat{S}^\dagger(r,\Phi), \tag{4}$$

where

$$\hat{\rho}_{th} = \prod_k \left[1 - e^{-\beta\hbar\omega_k}\right] e^{-\beta\hbar\omega_k \hat{b}_k^\dagger \hat{b}_k} \tag{5}$$

is the density matrix of the thermal bath, and

$$\hat{S}(r_k,\Phi_k) = \exp\left[r_k\left(\frac{\hat{b}_k^2}{2}e^{-i2\Phi_k} - \frac{\hat{b}_k^{\dagger 2}}{2}e^{i2\Phi_k}\right)\right] \tag{6}$$

is the squeezing operator with r_k, Φ_k being the squeezing parameters [46]. We are interested in the reduced dynamics of the 'open' system of interest S, which is obtained by tracing over the bath degrees of freedom. Using Eqs. (1), (3) in Eq. (2) and tracing over the bath variables, we obtain the reduced density matrix for S, in the system eigenbasis, as [36]

$$
\begin{aligned}
\rho_{nm}^s(t) = {}& e^{-\frac{i}{\hbar}(E_n - E_m)t} e^{-i(E_n^2 - E_m^2)\sum_k \frac{g_k^2}{\hbar^2\omega_k^2}\sin(\omega_k t)} \\
& \times \exp\left[-\frac{1}{2}(E_m - E_n)^2 \sum_k \frac{g_k^2}{\hbar^2\omega_k^2}\coth\left(\frac{\beta\hbar\omega_k}{2}\right)\right. \\
& \left. \times \left|(e^{i\omega_k t}-1)\cosh(r_k) + (e^{-i\omega_k t}-1)\sinh(r_k)e^{i2\Phi_k}\right|^2\right] \rho_{nm}^s(0).
\end{aligned}
\tag{7}
$$

From (7) we obtain the master equation as

$$\dot{\rho}_{nm}^s(t) = \left[-\frac{i}{\hbar}(E_n - E_m) + i\dot{\eta}(t)(E_n^2 - E_m^2) - (E_n - E_m)^2\dot{\gamma}(t)\right]\rho_{nm}^s(t), \tag{8}$$

where

$$\eta(t) = -\sum_k \frac{g_k^2}{\hbar^2\omega_k^2}\sin(\omega_k t), \tag{9}$$

and

$$\gamma(t) = \frac{1}{2}\sum_k \frac{g_k^2}{\hbar^2\omega_k^2}\coth\left(\frac{\beta\hbar\omega_k}{2}\right)\left|(e^{i\omega_k t}-1)\cosh(r_k) + (e^{-i\omega_k t}-1)\sinh(r_k)e^{i2\Phi_k}\right|^2. \tag{10}$$

For the case of an Ohmic bath with spectral density

$$I(\omega) = \frac{\gamma_0}{\pi}\omega e^{-\omega/\omega_c}, \tag{11}$$

where γ_0 and ω_c are bath parameters, $\eta(t)$ and $\gamma(t)$ can be evaluated [36] and we quote the results:

$$\eta(t) = -\frac{\gamma_0}{\pi}\tan^{-1}(\omega_c t), \tag{12}$$

and

$$
\begin{aligned}
\gamma(t) = {}& \frac{\gamma_0}{2\pi}\cosh(2r)\ln(1 + \omega_c^2 t^2) - \frac{\gamma_0}{4\pi}\sinh(2r)\ln\left[\frac{\left(1 + 4\omega_c^2(t-a)^2\right)}{\left(1 + \omega_c^2(t-2a)^2\right)^2}\right] \\
& -\frac{\gamma_0}{4\pi}\sinh(2r)\ln(1 + 4a^2\omega_c^2),
\end{aligned}
\tag{13}
$$

at $T = 0$, with $t > 2a$;

$$
\begin{aligned}
\gamma(t) &= \frac{\gamma_0 k_B T}{\pi \hbar \omega_c} \cosh(2r) \left[2\omega_c t \tan^{-1}(\omega_c t) + \ln\left(\frac{1}{1 + \omega_c^2 t^2}\right) \right] \\
&\quad - \frac{\gamma_0 k_B T}{2\pi \hbar \omega_c} \sinh(2r) \Bigg[4\omega_c(t - a)\tan^{-1}(2\omega_c(t - a)) \\
&\quad - 4\omega_c(t - 2a)\tan^{-1}(\omega_c(t - 2a)) + 4a\omega_c \tan^{-1}(2a\omega_c) \\
&\quad + \ln\left(\frac{\left[1 + \omega_c^2(t - 2a)^2\right]^2}{[1 + 4\omega_c^2(t - a)^2]}\right) + \ln\left(\frac{1}{1 + 4a^2\omega_c^2}\right) \Bigg],
\end{aligned}
\tag{14}
$$

for high T, and again with $t > 2a$. Here we have taken, for simplicity, the squeezed bath parameters as

$$
\begin{aligned}
\cosh\left(2r(\omega)\right) &= \cosh(2r), \quad \sinh\left(2r(\omega)\right) = \sinh(2r), \\
\Phi(\omega) &= a\omega,
\end{aligned}
\tag{15}
$$

where a is a constant depending upon the squeezed bath. We will make use of Eqs. (9), (10), (12), (13) and (14) in the subsequent analysis. Note that the results pertaining to a thermal bath can be obtained from the above equations by setting the squeezing parameters r and Φ to zero.

III.   QUANTUM PHASE DISTRIBUTION FOR AN OSCILLATOR SYSTEM

As discussed in the Introduction, it is more convenient to deal with the quantum phase distribution than a hermitian quantum phase operator. Following Agarwal *et al.* [35] we define a phase distribution $\mathcal{P}(\theta)$ for a given density operator ρ as

$$
\begin{aligned}
\mathcal{P}(\theta) &= \frac{1}{2\pi} \langle \theta | \rho | \theta \rangle, \ 0 \le \theta \le 2\pi, \\
&= \frac{1}{2\pi} \sum_{m,n=0}^{\infty} \rho_{m,n} e^{i(n-m)\theta},
\end{aligned}
\tag{16}
$$

where the states $|\theta\rangle$ are the eigenstates of the Susskind-Glogower [29] phase operator corresponding to eigenvalues of unit magnitude and are defined in terms of the number states $|n\rangle$ as

$$
|\theta\rangle = \sum_{n=0}^{\infty} e^{in\theta}|n\rangle.
\tag{17}
$$

The sum in Eq. (16) is assumed to converge. The phase distribution is positive definite and normalized to unity.

A.   System of a harmonic oscillator

For the case where the system S is a harmonic oscillator with the Hamiltonian

$$
H_S = \hbar\omega\left(a^\dagger a + \frac{1}{2}\right),
\tag{18}
$$

the number states serve as an appropriate basis for the system Hamiltonian and the system energy eigenvalue in this basis is

$$
E_n = \hbar\omega\left(n + \frac{1}{2}\right).
\tag{19}
$$

Using this in Eq. (7) we obtain

$$
\rho_{n,m}^s(t) = e^{-i\omega(n-m)t} e^{i(\hbar\omega)^2(n-m)(n+m+1)\eta(t)} e^{-(\hbar\omega)^2(n-m)^2\gamma(t)} \rho_{n,m}^s(0),
\tag{20}
$$

where $\eta(t)$ and $\gamma(t)$ are as in Eqs. (9) and (10), respectively.

The Hamiltonian described here has been used by Turchette *et al.* [26] to describe an experimental study of the decoherence and decay of quantum states of a trapped atomic ion's harmonic motion interacting with an engineered high-temperature 'phase reservoir', which is simulated by random variations in the trap frequency – changing the phase of the ion oscillation without changing its energy, i.e., adiabatically modulating the trap frequency. In such a system it would be interesting to construct the quantum phase distribution associated with the reduced density matrix of the system and obtain the dynamics of the phase distribution as the system evolves under the influence of its environment. Equation (20) when substituted in Eq. (16) provides us with the phase distribution of the harmonic oscillator system interacting with its environment via a QND type of interaction.

Now we obtain the phase distributions for some physically interesting initial conditions of our harmonic oscillator system S.

1. System initially in a coherent state

The initial density matrix of the system is

$$\rho^s(0) = |\alpha\rangle\langle\alpha|, \tag{21}$$

where

$$\alpha = |\alpha|e^{i\theta_0} \tag{22}$$

is a coherent state [47]. Thus the initial density matrix in the system basis is

$$\rho^s_{n,m}(0) = \langle n|\alpha\rangle\langle\alpha|m\rangle. \tag{23}$$

Now making use of the expansion of the coherent state in terms of the number states we get

$$\langle\alpha|n\rangle = \frac{|\alpha|^n}{\sqrt{n!}}e^{\frac{-|\alpha|^2}{2}}e^{-in\theta_0}. \tag{24}$$

It is to be noted that each of the diagonal elements of the above density matrix (23) is given by a Poisson distribution. Using Eq. (24) (and its complex conjugate) in Eq. (23), substituting it in Eq. (20), and then using Eq. (20) in Eq. (16) we obtain the phase distribution as

$$\mathcal{P}(\theta) = \frac{1}{2\pi}\sum_{m,n=0}^{\infty}\frac{|\alpha|^{n+m}}{\sqrt{n!m!}}e^{-|\alpha|^2}e^{-i(m-n)(\theta-\theta_0)}e^{-i\omega(m-n)t}$$
$$\times e^{i(\hbar\omega)^2(m-n)(n+m+1)\eta(t)}e^{-(\hbar\omega)^2(n-m)^2\gamma(t)}. \tag{25}$$

Figure 1 depicts the behavior of the quantum phase distribution, $\mathcal{P}(\theta)$ given by Eq. (25), as a function of θ (in radians) as it evolves under different environmental conditions. It can be clearly seen that in comparison with the unitary evolution (continuous curve), as the temperature T increases, the phase distribution broadens thereby indicating increasing phase diffusion with T. The phase diffusion also increases with an increase in the value of the squeezing parameter r, defined by (15), as is evident from a comparison of the large-dashed and the dot-dashed curves. Also by comparing the dot-dashed and double dot-dashed curves indicating the same environmental conditions but different evolution times t, it can be seen that an increase in exposure time to the environment causes a corresponding increase in phase diffusion. The broadening of the curves in all cases takes place in such a fashion that the normalization of the phase distribution function is preserved. For all the figures in this paper, we have set $\omega = 1.0$, $\omega_c = 100$, $|\alpha|^2 = 5$, $a = 0.0$, and θ_0 (Eq. (22)) = 0.

2. System initially in a squeezed coherent state

The initial density matrix of the system is

$$\rho^s(0) = |\xi,\alpha\rangle\langle\alpha,\xi|, \tag{26}$$

where the squeezed coherent state is defined as [47]

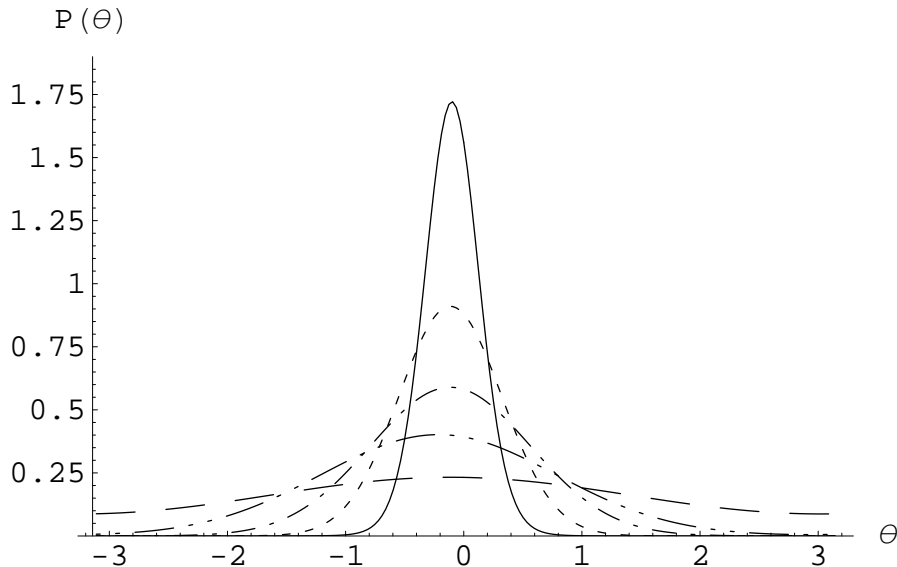$$|\xi,\alpha\rangle = S(\xi)D(\alpha)|0\rangle. \tag{27}$$

FIG. 1: Quantum phase distribution, $\mathcal{P}(\theta)$ given by Eq. (25), for a harmonic oscillator initially in a coherent state, as a function of θ (in radians), for different environmental conditions and evolution times. The parameters have been taken as $\omega = 1.0$, $\omega_c = 100$, $|\alpha|^2 = 5$, $a = 0.0$, $\gamma_0 = 0.0025$. The small-dashed and the large-dashed curves are for temperatures T (in units with $\hbar \equiv k_B \equiv 1$) = 0 and 300, respectively, with an environmental squeezing parameter $r = 2$ and at an evolution time $t = 0.1$. The dot-dashed and the double dot-dashed curves are at evolution times $t = 0.1$ and 0.2, respectively, for $T = 300$ and $r = 1$. The continuous curve represents unitary evolution ($\gamma_0 = 0$).

Here S denotes the standard squeezing operator and D denotes the standard displacement operator [47]. The initial density matrix (26) in the system basis is

$$
\begin{aligned}
\rho_{m,n}^s(0) &= \langle m|\rho^s(0)|n\rangle \\
&= \frac{e^{i\frac{\psi}{2}(m-n)}}{2^{\frac{(m+n)}{2}}\sqrt{m!n!}} \frac{(\tanh(r_1))^{\frac{(m+n)}{2}}}{\cosh(r_1)} \exp\left[-|\alpha|^2(1-\tanh(r_1)\cos(2\theta_0-\psi))\right] \\
&\quad \times H_m\left[\frac{|\alpha|e^{i(\theta_0-\frac{\psi}{2})}}{\sqrt{\sinh(2r_1)}}\right] H_n^*\left[\frac{|\alpha|e^{i(\theta_0-\frac{\psi}{2})}}{\sqrt{\sinh(2r_1)}}\right],
\end{aligned}
\tag{28}
$$

where $\xi = r_1 e^{i\psi}$. Here $H_n[z]$ is a Hermite polynomial. Using Eq. (28) in Eq. (20) and substituting it in Eq. (16) we obtain the phase distribution as

$$
\begin{aligned}
\mathcal{P}(\theta) &= \frac{1}{2\pi}\sum_{m,n=0}^{\infty} e^{i(n-m)\theta} \frac{e^{i\frac{\psi}{2}(m-n)}}{2^{\frac{(m+n)}{2}}\sqrt{m!n!}} \frac{(\tanh(r_1))^{\frac{(m+n)}{2}}}{\cosh(r_1)} \\
&\quad \times \exp\left[-|\alpha|^2(1-\tanh(r_1)\cos(2\theta_0-\psi))\right] \\
&\quad \times H_m\left[\frac{|\alpha|e^{i(\theta_0-\frac{\psi}{2})}}{\sqrt{\sinh(2r_1)}}\right] H_n^*\left[\frac{|\alpha|e^{i(\theta_0-\frac{\psi}{2})}}{\sqrt{\sinh(2r_1)}}\right] \\
&\quad \times e^{-i\omega(m-n)t} e^{i(\hbar\omega)^2(m-n)(n+m+1)\eta(t)} e^{-(\hbar\omega)^2(n-m)^2\gamma(t)}.
\end{aligned}
\tag{29}
$$

Figure 2 clearly indicates an increase in phase diffusion, corresponding to a broadening of the phase distribution curve, with an increase in T or bath squeezing parameter r or evolution time t, as was the case in Fig. 1. An interesting difference can be seen in the phase distribution curves corresponding to unitary evolution (continuous curves) in Figs. 1 and 2, viz., the continuous curve in Fig. 2 is more tilted than that in Fig. 1. This is due to the squeezing inherent in the initial state of the system (26) which is quantified by the parameters r_1 and ψ.
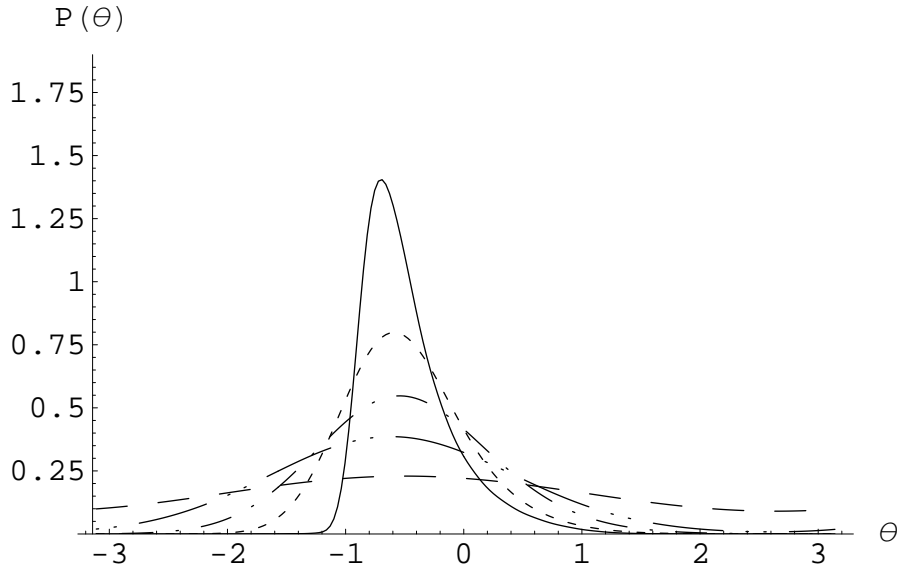
FIG. 2: Quantum phase distribution, $\mathcal{P}(\theta)$ given by Eq. (29), for a harmonic oscillator initially in a squeezed coherent state, as a function of θ (in radians), for different environmental conditions and evolution times. The parameters have been taken as $\omega = 1.0$, $|\alpha|^2 = 5$, $a = 0.0$, $\gamma_0 = 0.0025$; $r_1 = 0.5$, and $\psi = \pi/4$ (r_1 and ψ are the system squeezing parameters (26)). The small-dashed and the large-dashed curves are for temperatures T (in units with $\hbar \equiv k_B \equiv 1$) $= 0$ and 300, respectively, at an environmental squeezing parameter (15) $r = 2$ and evolution time $t = 0.1$. The dot-dashed and the double dot-dashed curves are at evolution times $t = 0.1$ and 0.2, respectively, with $T = 300$ and $r = 1$. The continuous curve represents unitary evolution ($\gamma_0 = 0$).

B. System of an anharmonic oscillator

Here we take up the case where the system is modelled as an anharmonic oscillator with the Hamiltonian

$$H_S = \hbar\omega\left(a^\dagger a + \frac{1}{2}\right) + \frac{\hbar\lambda}{2}(a^\dagger)^2 a^2. \tag{30}$$

This has been used, for example, in studies related to a non-absorbing Kerr medium interacting with a single mode of the quantized electromagnetic field [37, 38]. In such a context λ is related to the third-order susceptibility of the Kerr medium [48]. The above Hamiltonian can be expressed (up to constant factors) in terms of the generators K_0, K_+ and K_- of the $SU(1,1)$ group. These generators have the following bosonic representation:

$$K_0 = \frac{1}{4}(a^\dagger a + a a^\dagger), \ \ K_+ = \frac{1}{2}(a^\dagger)^2, \ \ K_- = \frac{1}{2}(a)^2. \tag{31}$$

In terms of these generators, Eq. (30) can be expressed as

$$H_S = 2\hbar\omega K_0 + 2\hbar\lambda K_+ K_-. \tag{32}$$

We make use of the unitary irreducible representations of the group $SU(1,1)$ known as the positive discrete series $\mathcal{D}^+(k)$, where k is the so called Bargmann index [49], such that the eigenvalue of the Casimir operator of the group is $k(k-1)$. This gives the value of k to be $\frac{1}{4}$ or $\frac{3}{4}$ [50, 51]. The case of $k = \frac{1}{4}$ marks the even sector of the representation with the vacuum state in this representation coinciding with the vacuum state of the harmonic oscillator, while the case of $k = \frac{3}{4}$ marks the odd sector of the representation. Thus the even and the odd sectors of the representation together span the number states [52]. The basis for this representation obeys the following properties:

$$\begin{aligned} K_0|m,k\rangle &= (m+k)|m,k\rangle, \\ K_+|m,k\rangle &= \sqrt{[(m+1)(m+2k)]}|m+1,k\rangle, \\ K_-|m,k\rangle &= \sqrt{[m(m+2k-1)]}|m-1,k\rangle, \end{aligned} \tag{33}$$

where $m = 0, 1, 2, \ldots$. Using the above properties of the generators, the action of H_S (30) on the basis of this representation is found to be

$$\begin{aligned} H_S|m,k\rangle &= 2\hbar\left[\omega(m+k) + \lambda m(m+2k-1)\right]|m,k\rangle \\ &= E_{m_k}|m,k\rangle. \end{aligned} \tag{34}$$

We use the above equation in Eq. (7) to obtain the reduced density matrix of the system S in the system basis $|m, k\rangle$ as

$$
\begin{aligned}
\rho^s_{m_k,n_k}(t) &= e^{-2i(m-n)[\omega+\lambda(m+n+2k-1)]t} \\
&\times e^{4i\hbar^2(m-n)[\omega+\lambda(m+n+2k-1)]\left[\omega(n+m+2k)+\lambda(n^2+m^2+(2k-1)(m+n))\right]\eta(t)} \\
&\times e^{-4\hbar^2(m-n)^2[\omega+\lambda(m+n+2k-1)]^2\gamma(t)}\rho^s_{m_k,n_k}(0).
\end{aligned}
\tag{35}
$$

Now let us consider some physically interesting initial conditions for our anharmonic oscillator system S.

1. System initially in a Kerr state

An initial Kerr state $|\psi_K\rangle$ [37] can be obtained as a result of an interaction of the usual coherent state of the electromagnetic field with a nonlinear Kerr medium mediated by the Hamiltonian H_S given in Eq. (30). This state is defined in terms of the number states as

$$
|\psi_K\rangle = \sum_n q_n |n\rangle,
\tag{36}
$$

where

$$
q_n = \frac{\alpha^n}{\sqrt{n!}} e^{\frac{-|\alpha|^2}{2}} e^{-i\chi n(n-1)}.
\tag{37}
$$

Here $|n\rangle$ represents the usual number state and $\chi = \frac{\lambda L}{2v}$, where λ is as in Eq. (30), L is the length of the medium and v is the speed of light in the Kerr medium in which the interaction has taken place. Thus the initial system density matrix is

$$
\begin{aligned}
\rho^s_{m_k,n_k}(0) &= \langle m, k|\psi_K\rangle\langle\psi_K|n, k\rangle \\
&= q_{2m}q^*_{2n} \quad \text{for} \quad k = \frac{1}{4} \\
&= q_{2m+1}q^*_{2n+1} \quad \text{for} \quad k = \frac{3}{4},
\end{aligned}
\tag{38}
$$

because the state $|m, k\rangle$ with $k = \frac{1}{4}$ represents an even number state while the state $|m, k\rangle$ for $k = \frac{3}{4}$ represents an odd number state. The phase distribution is obtained by substituting Eq. (38) in Eq. (35) and then in Eq. (16), making use of the fact that for the positive discrete series representation of the group $SU(1, 1)$, the even and the odd sectors together span the number states:

$$
\begin{aligned}
\mathcal{P}(\theta) &= \frac{1}{2\pi} \sum_{m,n=0}^{\infty} q_{2m}q^*_{2n} e^{i2(n-m)\theta} e^{-2i(m-n)\left[\omega+\lambda(m+n-\frac{1}{2})\right]t} \\
&\times e^{4i\hbar^2(m-n)\left[\omega+\lambda(m+n-\frac{1}{2})\right]\left[\omega(n+m+\frac{1}{2})+\lambda(n^2+m^2-\frac{1}{2}(m+n))\right]\eta(t)} \\
&\times e^{-4\hbar^2(m-n)^2\left[\omega+\lambda(m+n-\frac{1}{2})\right]^2\gamma(t)} \\
&+ \frac{1}{2\pi} \sum_{m,n=0}^{\infty} q_{2m+1}q^*_{2n+1} e^{i2(n-m)\theta} e^{-2i(m-n)\left[\omega+\lambda(m+n+\frac{1}{2})\right]t} \\
&\times e^{4i\hbar^2(m-n)\left[\omega+\lambda(m+n+\frac{1}{2})\right]\left[\omega(n+m+\frac{3}{2})+\lambda(n^2+m^2+\frac{1}{2}(m+n))\right]\eta(t)} \\
&\times e^{-4\hbar^2(m-n)^2\left[\omega+\lambda(m+n+\frac{1}{2})\right]^2\gamma(t)}.
\end{aligned}
\tag{39}
$$

q_{2m}, q_{2m+1} can be obtained from Eq. (37).

Figures 3 and 4 represent the evolution of the quantum phase distribution, $\mathcal{P}(\theta)$ given by Eq. (39), as a function of θ for an anharmonic oscillator system (30) starting from an initial Kerr state (36). While Fig. 3 represents the evolution for a fixed evolution time but different environmental conditions, Fig. 4 represents different evolution times under the same environmental conditions. From Fig. 3 it is evident that increasing the temperature T causes a broadening of the phase distributions. Increased phase diffusion also results from an increase in environmental squeezing r. Figure 4 clearly shows that with an increase in the evolution time t, i.e., an increase in exposure to the environment, the quantum phase distribution shifts as well as diffuses. A similar conclusion was obtained by Agarwal *et al.* [35] for an analogous situation studied under unitary evolution.
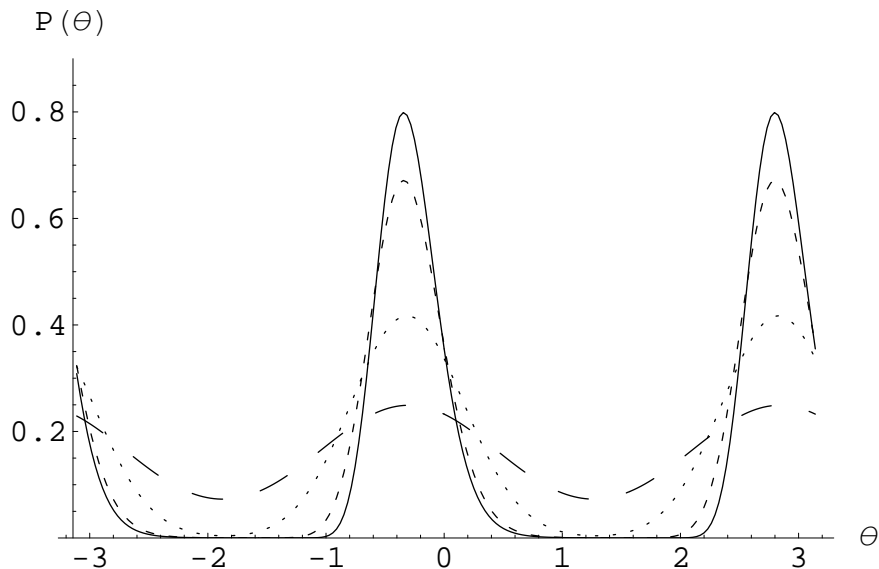
FIG. 3: Quantum phase distribution, $\mathcal{P}(\theta)$ given by Eq. (39), for an anharmonic oscillator initially in a Kerr state, as a function of θ (in radians), for different environmental conditions at a fixed time of evolution. The parameters have been taken as $\gamma_0 = 0.0025$, $|\alpha|^2 = 5$, $\omega = 1.0$, $\chi = \lambda = 0.02$ and evolution time $t = 0.1$. The small-dashed and the large-dashed curves are for the bath squeezing parameter $r = 0$ and 2, respectively, at T (in units with $\hbar \equiv k_B \equiv 1$) = 50. The dotted curve is for $T = 0$ and $r = 2$. The continuous curve represents unitary evolution ($\gamma_0 = 0$).
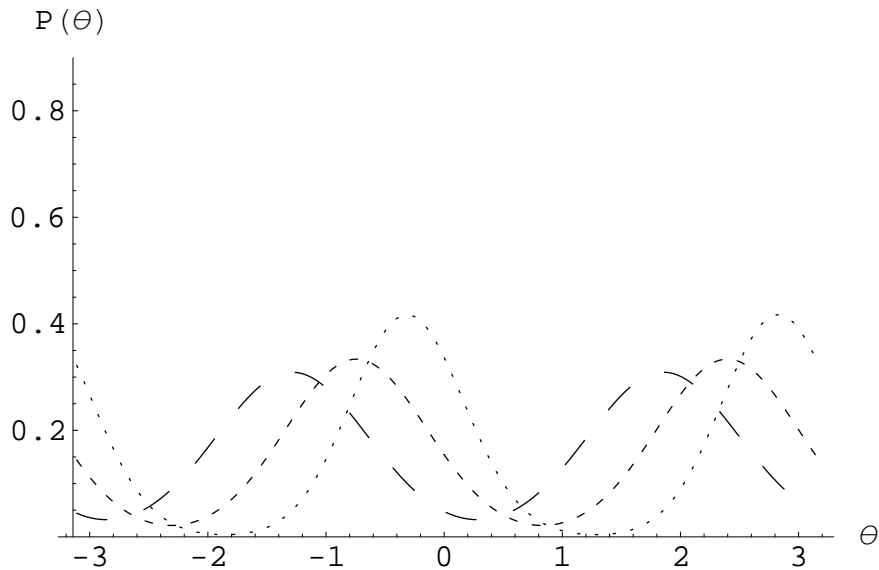

FIG. 4: Time evolution of the quantum phase distribution, $\mathcal{P}(\theta)$ given by Eq. (39), for an anharmonic oscillator initially in a Kerr state, as a function of θ (in radians), for different evolution times under fixed environmental conditions. The parameters have been taken as $\gamma_0 = 0.0025$, $|\alpha|^2 = 5$, $\omega = 1.0$, $\chi = \lambda = 0.02$ (as in Fig. 3), $T = 0$, and $r = 2$. The dotted curve is for an evolution time $t = 0.1$, the small-dashed curve is for $t = 0.5$, and the large-dashed curve is for $t = 1.0$.

2. System initially in a squeezed Kerr state

A squeezed Kerr state [37] is defined in terms of the number states as

$$|\psi_{SK}\rangle = \sum_m s_m |m\rangle. \tag{40}$$

Thus the initial system density matrix in the system basis $|m, k\rangle$ (34) is

$$\rho^s_{m_k, n_k}(0) = \langle m, k|\psi_{SK}\rangle\langle\psi_{SK}|n, k\rangle$$

$$= s_{2m}s_{2n}^* \quad \text{for} \quad k = \frac{1}{4}$$

$$= s_{2m+1}s_{2n+1}^* \quad \text{for} \quad k = \frac{3}{4}. \tag{41}$$

Here

$$s_{2m} = \sum_p q_{2p}G_{2m2p}(z), \tag{42}$$

and

$$s_{2m+1} = \sum_p q_{2p+1}G_{2m+12p+1}(z), \tag{43}$$

with $z = r_1 e^{i\phi}$, and $G_{mp}(z) = \langle m|S(z)|p\rangle$, where $S(z)$ is the usual squeezing operator, is given by [53]

$$\begin{aligned} G_{2m2p} &= \frac{(-1)^p}{p!m!}\left(\frac{(2p)!(2m)!}{\cosh(r_1)}\right)^{\frac{1}{2}}\exp\left(i(m-p)\phi\right) \\ &\times \left(\frac{\tanh(r_1)}{2}\right)^{(m+p)}F_1^2\left[-p,-m;\frac{1}{2};-\frac{1}{(\sinh(r_1))^2}\right]. \end{aligned} \tag{44}$$

Similarly, $G_{2m+12p+1}(z)$ is given by

$$\begin{aligned} G_{2m+12p+1} &= \frac{(-1)^p}{p!m!}\left(\frac{(2p+1)!(2m+1)!}{\cosh^3(r_1)}\right)^{\frac{1}{2}}\exp\left(i(m-p)\phi\right) \\ &\times \left(\frac{\tanh(r_1)}{2}\right)^{(m+p)}F_1^2\left[-p,-m;\frac{3}{2};-\frac{1}{(\sinh(r_1))^2}\right]. \end{aligned} \tag{45}$$

Here F_1^2 is the Gauss hypergeometric function [54]. We make use of even p in Eqs. (42), (44), and odd p in Eqs. (43), (45), because as has been pointed out in [53], G_{mn} is nonzero only for m, n either both even or both odd. Since m is even in (42), it follows that p too should be even, and similarly for (43) where m is odd. For convenience, it is sometimes assumed that ϕ is zero and $z = r_1$ is real. Using Eqs. (42), (43), (44) and (45) in Eq. (41), substituting it in Eq. (35) and then in Eq. (16) we obtain the phase distribution function as

$$\begin{aligned} \mathcal{P}(\theta) &= \frac{1}{2\pi}\sum_{m,n=0}^{\infty}s_{2m}s_{2n}^*e^{i2(n-m)\theta}e^{-2i(m-n)\left[\omega+\lambda(m+n-\frac{1}{2})\right]t} \\ &\times e^{4i\hbar^2(m-n)\left[\omega+\lambda(m+n-\frac{1}{2})\right]\left[\omega(n+m+\frac{1}{2})+\lambda(n^2+m^2-\frac{1}{2}(m+n))\right]\eta(t)} \\ &\times e^{-4\hbar^2(m-n)^2\left[\omega+\lambda(m+n-\frac{1}{2})\right]^2\gamma(t)} \\ &+ \frac{1}{2\pi}\sum_{m,n=0}^{\infty}s_{2m+1}s_{2n+1}^*e^{i2(n-m)\theta}e^{-2i(m-n)\left[\omega+\lambda(m+n+\frac{1}{2})\right]t} \\ &\times e^{4i\hbar^2(m-n)\left[\omega+\lambda(m+n+\frac{1}{2})\right]\left[\omega(n+m+\frac{3}{2})+\lambda(n^2+m^2+\frac{1}{2}(m+n))\right]\eta(t)} \\ &\times e^{-4\hbar^2(m-n)^2\left[\omega+\lambda(m+n+\frac{1}{2})\right]^2\gamma(t)}. \end{aligned} \tag{46}$$

Here s_{2m} is as in Eq. (42) and s_{2m+1} is as in Eq. (43).

Figure 5 depicts the evolution of the quantum phase distribution, $\mathcal{P}(\theta)$ given by Eq. (46), as a function of θ for an anharmonic oscillator system (30) starting from an initial squeezed Kerr state (40). The environmental effects are clearly depicted in that an increase in temperature T and squeezing parameter r results in the broadening of the phase distribution indicating increased phase diffusion. In the same figure, a drastic influence of the environment on the unitary behavior can be seen from the sharp fall in the amplitude of the phase distribution with the inclusion of environmental effects. A comparison between the unitary evolutions (continuous curves) of Figs. 3 and 5 highlights the difference in the initial conditions of the system depicted in these curves. The peak amplitude of the unitary evolution (continuous curve) is greater in case of a system initially in a squeezed Kerr state (Fig. 5) than that in a Kerr state (Fig. 3). This is indicative of the additional squeezing in the initial state for Fig. 5. The corresponding narrowing of the peaks in Fig. 5 is due to the fact that the phase distributions are normalized. Note that the multiple peaks are a common feature of the quantum phase distributions of the anharmonic oscillator system (30) as opposed to the single peaks of the harmonic oscillator system (18).
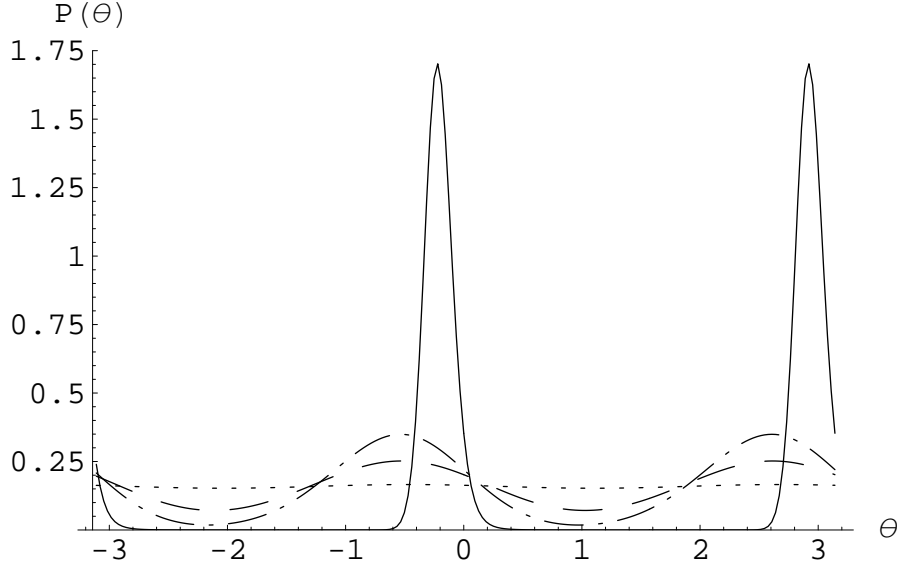
FIG. 5: Quantum phase distribution, $\mathcal{P}(\theta)$ given by Eq. (46), for an anharmonic oscillator initially in a squeezed Kerr state, as a function of θ (in radians), for different environmental conditions. The parameters have been taken as $t = 0.1$, $\chi = \lambda = 0.02$, $\gamma_0 = 0.025$, $r_1 = 0.4$ and $\phi = 0$ (r_1, ϕ are the system squeezing parameters). The dot-dashed and the dotted curves are for T (in units with $\hbar \equiv k_B \equiv 1$) $= 0$ and 100, respectively, with the environmental squeezing parameter $r = 1$. The large-dashed curve is at $T = 100$ and $r = 0$. The continuous curve represents the unitary evolution ($\gamma_0 = 0$).

IV.   QUANTUM PHASE DISTRIBUTION OF A TWO-LEVEL ATOMIC SYSTEM

In this section we discuss the case where our system S is a two-level atom with a representation of the group $SU(2)$. The system Hamiltonian, to be substituted in Eq. (1), is

$$H_S = \frac{\hbar\omega}{2}\sigma_Z, \tag{47}$$

where σ_Z is the usual Pauli matrix (as has been used, for example, in the quantum computation models in [39, 40, 41]). The Wigner-Dicke states [43, 44, 55] $|j, m\rangle$, which are the simultaneous eigenstates of the angular momentum operators J^2 and J_Z, serve as the basis states for H_S and we have

$$\begin{aligned} H_S|j, m\rangle &= \hbar\omega m|j, m\rangle \\ &= E_{j,m}|j, m\rangle. \end{aligned} \tag{48}$$

Here $-j \leq m \leq j$. Using this basis and the above equation in Eq. (7) we obtain the reduced density matrix of the system as

$$\begin{aligned} \rho^s_{jm,jn}(t) &= e^{-i\omega(m-n)t}e^{i(\hbar\omega)^2(m^2-n^2)\eta(t)} \\ &\quad \times e^{-(\hbar\omega)^2(m-n)^2\gamma(t)}\rho^s_{jm,jn}(0). \end{aligned} \tag{49}$$

Following Agarwal and Singh [42] we introduce the phase distribution $\mathcal{P}(\phi)$, ϕ being related to the phase of the dipole moment of the system, as

$$\mathcal{P}(\phi) = \frac{2j+1}{4\pi}\int_0^\pi d\theta \sin\theta \, Q(\theta, \phi), \tag{50}$$

where $\mathcal{P}(\phi) > 0$ and is normalized to unity, i.e., $\int_0^{2\pi} d\phi \mathcal{P}(\phi) = 1$. Here $Q(\theta, \phi)$ is defined as

$$Q(\theta, \phi) = \langle\theta, \phi|\rho^s|\theta, \phi\rangle, \tag{51}$$

where $|\theta, \phi\rangle$ are the atomic coherent states [56, 57] given by an expansion over the Wigner-Dicke states [44] as

$$|\theta, \phi\rangle = \sum_{m=-j}^{j} \binom{2j}{j+m}^{\frac{1}{2}} (\sin(\theta/2))^{j+m}(\cos(\theta/2))^{j-m}|j, m\rangle e^{-i(j+m)\phi}. \tag{52}$$

Using Eq. (51) in Eq. (50), with insertions of partitions of unity in terms of the Wigner-Dicke states, we can write the phase distribution function as

$$
\begin{aligned}
\mathcal{P}(\phi) \;=\; & \frac{2j+1}{4\pi} \int_0^\pi d\theta \sin\theta \sum_{n,m=-j}^{j} \langle \theta, \phi | j, n \rangle \\
& \times \langle j, n | \rho^s(t) | j, m \rangle \langle j, m | \theta, \phi \rangle.
\end{aligned}
\tag{53}
$$

We make use of Eq. (49) and

$$
\langle j, m | \theta, \phi \rangle = \binom{2j}{j+m}^{\frac{1}{2}} (\sin(\theta/2))^{j+m} (\cos(\theta/2))^{j-m} e^{-i(j+m)\phi}
\tag{54}
$$

and its conjugate in Eq. (53) to obtain the required phase distribution for specific initial conditions of the system S. Let us now consider some physically interesting initial conditions for the two-level system S.

A. System initially in a Wigner-Dicke state

A Wigner-Dicke state is the atomic analogue of the Fock state [44]. The initial density matrix of the system S in this case is

$$
\rho^s(0) = |j, \tilde{m}\rangle\langle j, \tilde{m}|,
\tag{55}
$$

which gives

$$
\langle j, n | \rho^s(t) | j, m \rangle = \delta_{n,\tilde{m}} \delta_{\tilde{m},m}.
\tag{56}
$$

Using this, the phase distribution becomes

$$
\mathcal{P}(\phi) = \frac{2j+1}{2\pi} \binom{2j}{j+\tilde{m}} B\left[j+\tilde{m}+1, j-\tilde{m}+1\right].
\tag{57}
$$

Here B stands for the Beta function. It is evident from Eq. (57) that the phase distribution for the atomic system starting in a Wigner-Dicke state is uniform and is independent of any bath dynamics. Here, since we have only one two-level system in Eq. (47), $j = \frac{1}{2}$ and $\mathcal{P}(\phi)$ can be seen to go over to $\frac{1}{2\pi}$, i.e., a uniform distribution.

B. System initially in an atomic coherent state

An atomic coherent state is the atomic analogue of the Glauber coherent state [44]. The initial density matrix of the system S in this case is

$$
\rho^s(0) = |\alpha, \beta\rangle\langle\alpha, \beta|
\tag{58}
$$

yielding the following matrix element in the $|j, m\rangle$ basis:

$$
\begin{aligned}
\langle j, n | \rho^s(t) | j, m \rangle \;=\; & e^{-i\omega(n-m)t} e^{i(\hbar\omega)^2(n^2-m^2)\eta(t)} \\
& \times e^{-(\hbar\omega)^2(n-m)^2\gamma(t)} \langle j, n | \alpha, \beta \rangle \langle \alpha, \beta | j, m \rangle.
\end{aligned}
\tag{59}
$$

Using Eqs. (59), (54) in Eq. (53) we obtain the phase distribution as

$$
\begin{aligned}
\mathcal{P}(\phi) \;=\; & \frac{2j+1}{4\pi} \int_0^\pi d\theta \sin\theta \sum_{n,m=-j}^{j} \binom{2j}{j+n}\binom{2j}{j+m} \\
& \times (\sin(\theta/2))^{2j+n+m} (\cos(\theta/2))^{2j-n-m} e^{-i(n-m)\beta} \\
& \times (\sin(\alpha/2))^{2j+n+m} (\cos(\alpha/2))^{2j-n-m} \\
& \times e^{-i\omega(n-m)t} e^{i(\hbar\omega)^2(n^2-m^2)\eta(t)} \\
& \times e^{-(\hbar\omega)^2(n-m)^2\gamma(t)} e^{i(n-m)\phi}.
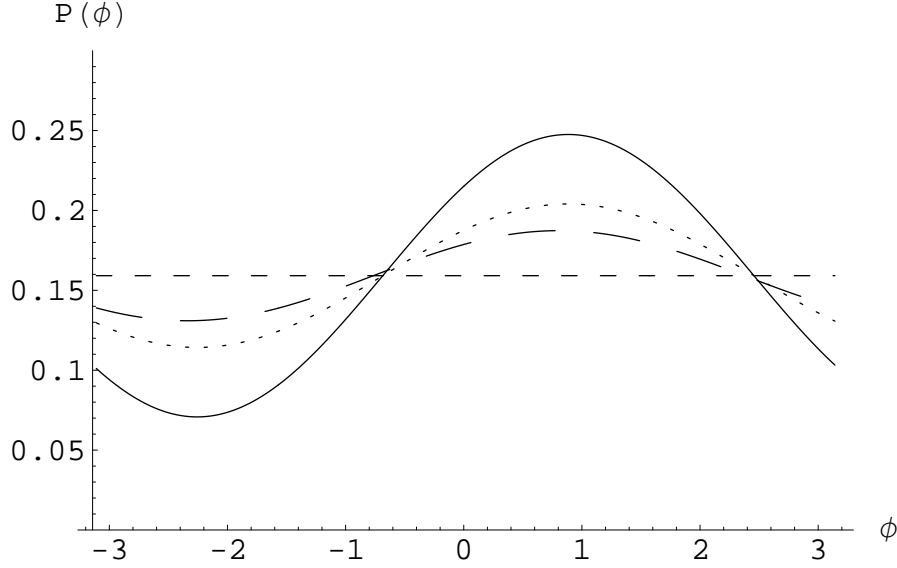\end{aligned}
\tag{60}
$$

FIG. 6: Quantum phase distribution, $\mathcal{P}(\phi)$ given by Eq. (62), for a two-level atom initially in an atomic coherent state, as a function of ϕ (in radians), for different environmental conditions and evolution times. The parameters have been taken as $\alpha = \beta = \pi/4$ [Eq. (58)], and $\gamma_0 = 0.025$. The continuous curve and the dotted curve are for the bath squeezing parameter $r = 0$ and 2, respectively, at a temperature $T = 0$ and an evolution time $t = 0.1$. The small-dashed and the large-dashed curves correspond to evolution times $t = 0.1$ and 0.02, respectively, at T (in units with $\hbar \equiv k_B \equiv 1$) $= 300$ and $r = 2$.

In the above equation, the θ integral can be carried out to yield

$$
\begin{aligned}
\mathcal{P}(\phi) = {} & \frac{2j+1}{2\pi} \sum_{n,m=-j}^{j} \binom{2j}{j+n}\binom{2j}{j+m} \frac{\Gamma(j+\frac{1}{2}(n+m)+1)\Gamma(j-\frac{1}{2}(n+m)+1)}{\Gamma(2j+2)} \\
& \times e^{-i(n-m)\beta}(\sin(\alpha/2))^{2j+n+m}(\cos(\alpha/2))^{2j-n-m} \\
& \times e^{-i\omega(n-m)t}e^{i(\hbar\omega)^2(n^2-m^2)\eta(t)} \\
& \times e^{-(\hbar\omega)^2(n-m)^2\gamma(t)}e^{i(n-m)\phi}.
\end{aligned}
\tag{61}
$$

Here Γ is the standard Gamma function. Since H_S given by Eq. (47) represents a single two-level atom, $j = \frac{1}{2}$. Eq. (61) is thus considerably simplified and we obtain the phase distribution as

$$
\mathcal{P}(\phi) = \frac{1}{2\pi}\left[1 + \frac{\pi}{4}\sin\alpha\cos(\beta+\omega t-\phi)e^{-(\hbar\omega)^2\gamma(t)}\right].
\tag{62}
$$

It can be easily checked that this $\mathcal{P}(\phi)$ is normalized to unity. As can be seen from Eq. (62), only $\gamma(t)$ plays a role in carrying the effect of the environment on the phase distribution. For a generic QND open quantum system described by (1), it can be shown that $\dot\gamma(t)$ is the decoherence causing term [36]. Thus Eq. (62) is a simple and neat formula clearly illustrating the effect of the environment on phase diffusion. By making use of $\gamma(t)$ from Eqs. (13) and (14) for $T = 0$ and for high T, respectively, we find that the second term on the right-hand side of Eq. (62) has a power-law decay at zero T and an exponential decay at high T, and eventually the phase distribution tends to the uniform limit of $\frac{1}{2\pi}$. Thus the effect of the environment stays for a longer time at zero T as compared to that at high T.

Figure 6 depicts the evolution of the quantum phase distribution, $\mathcal{P}(\phi)$ given by Eq. (62), as a function of ϕ (in radians) for different environmental conditions. It is clearly seen that increasing the temperature T, the bath squeezing parameter r, and the environment exposure time t cause a broadening of the phase distribution curve, indicating an increase of phase diffusion. The broadening of the curves preserves the normalization of the phase distribution.

C. System initially in an atomic squeezed state

An atomic squeezed state [45, 56, 57, 58] is expressed in terms of the Wigner-Dicke states as

$$
|\zeta, p\rangle = A_p \exp(\Theta\hat{J}_Z)\exp(-i\frac{\pi}{2}\hat{J}_Y)|j, p\rangle,
\tag{63}
$$

where

$$e^{2\Theta} = \tanh(2|\zeta|), \tag{64}$$

with ζ indicating the initial squeezing of the system. The initial density matrix of the system S in this case is

$$\rho^s(0) = |\zeta, p\rangle\langle\zeta, p|. \tag{65}$$

Using Eq. (53) along with the expressions

$$\begin{aligned}
\langle j, n|\rho^s(t)|j, m\rangle &= e^{-i\omega(n-m)t}e^{i(\hbar\omega)^2(n^2-m^2)\eta(t)} \\
&\times e^{-(\hbar\omega)^2(n-m)^2\gamma(t)}\langle j, n|\zeta, p\rangle\langle\zeta, p|j, m\rangle,
\end{aligned} \tag{66}$$

and

$$\langle j, n|\zeta, p\rangle = A_p e^{n\Theta}d_{np}^j\left(\frac{\pi}{2}\right), \tag{67}$$

[56], where $d_{np}^j(\frac{\pi}{2})$ is the standard Wigner symbol for the rotation operator [59]:

$$d_{np}^j\left(\frac{\pi}{2}\right) = \langle j, n|e^{-i\frac{\pi}{2}J_Y}|j, p\rangle, \tag{68}$$

and

$$|A_p|^2 = \left(\sum_r \frac{(-1)^r(2j-r)!(\cosh\Theta)^{2j-2r}}{r!(j+p-r)!(j-p-r)!}\right)^{-1}, \tag{69}$$

we obtain the phase distribution function as

$$\begin{aligned}
\mathcal{P}(\phi) &= \frac{2j+1}{4\pi}|A_p|^2\int_0^\pi d\theta\sin\theta\sum_{n,m=-j}^j\binom{2j}{j+n}^{\frac{1}{2}}\binom{2j}{j+m}^{\frac{1}{2}} \\
&\times(\sin(\theta/2))^{2j+n+m}(\cos(\theta/2))^{2j-n-m}e^{i(n-m)\phi} \\
&\times e^{-i\omega(n-m)t}e^{i(\hbar\omega)^2(n^2-m^2)\eta(t)} \\
&\times e^{-(\hbar\omega)^2(n-m)^2\gamma(t)}e^{(n+m)\Theta}d_{np}^j\left(\frac{\pi}{2}\right)d_{mp}^{*j}\left(\frac{\pi}{2}\right).
\end{aligned} \tag{70}$$

In Eq. (70) the θ integral can be carried out to yield

$$\begin{aligned}
\mathcal{P}(\phi) &= \frac{2j+1}{2\pi}|A_p|^2\sum_{n,m=-j}^j\binom{2j}{j+n}^{\frac{1}{2}}\binom{2j}{j+m}^{\frac{1}{2}}\frac{\Gamma(j+\frac{1}{2}(n+m)+1)\Gamma(j-\frac{1}{2}(n+m)+1)}{\Gamma(2j+2)} \\
&\times e^{i(n-m)\phi}e^{-i\omega(n-m)t}e^{i(\hbar\omega)^2(n^2-m^2)\eta(t)} \\
&\times e^{-(\hbar\omega)^2(n-m)^2\gamma(t)}e^{(n+m)\Theta}d_{np}^j\left(\frac{\pi}{2}\right)d_{mp}^{*j}\left(\frac{\pi}{2}\right).
\end{aligned} \tag{71}$$

As discussed in subsection IVB above, for a single two-level system, $j = \frac{1}{2}$. We take up two cases for the two values of p appearing in Eq. (63): $p = -\frac{1}{2}$ called the south pole of the phase space of the two-level system, and $p = \frac{1}{2}$ called the north pole of the phase space [45].

a. South pole ($p = -\frac{1}{2}$):

The phase distribution in Eq. (71) is considerably simplified to give

$$\mathcal{P}(\phi) = \frac{1}{2\pi}\left[1 - \frac{\pi}{4\cosh\Theta}\cos(\phi - \omega t)e^{-(\hbar\omega)^2\gamma(t)}\right]. \tag{72}$$

b. North pole ($p = \frac{1}{2}$):

Eq. (71) is simplified to give

$$\mathcal{P}(\phi) = \frac{1}{2\pi}\left[1 + \frac{\pi}{4\cosh\Theta}\cos(\phi - \omega t)e^{-(\hbar\omega)^2\gamma(t)}\right]. \tag{73}$$
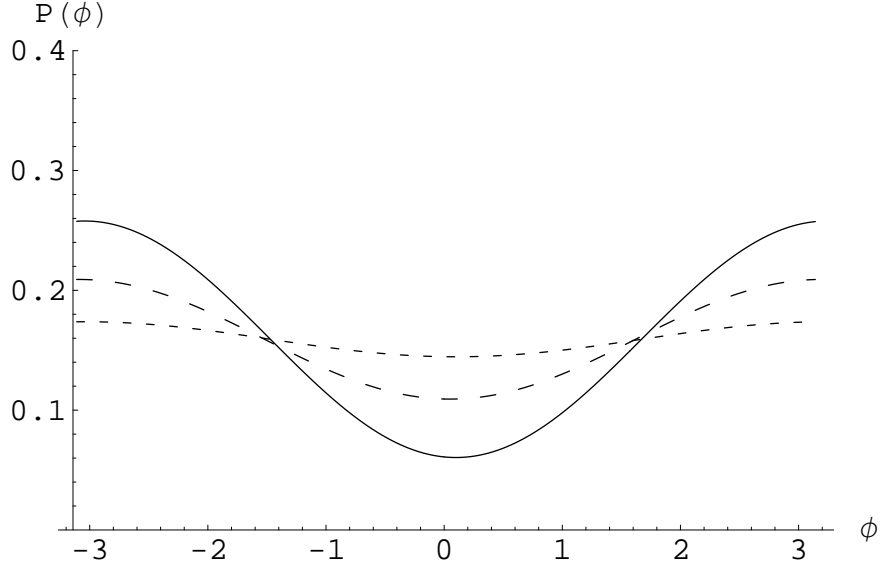
FIG. 7: Quantum phase distribution, $\mathcal{P}(\phi)$ given by Eq. (72), at the south pole of the phase space for a two-level atom initially in an atomic squeezed state, as a function of ϕ (in radians), for different environmental conditions. The system squeezing parameter (64) Θ is taken as = - 0.5494, the bath squeezing parameter $r = 1$, and $\gamma_0 = 0.025$. The continuous curve corresponds to a temperature $T = 0$ and an evolution time $t = 0.1$, while the small-dashed and large-dashed curves correspond to evolution times $t = 0.1$ and 0.05, respectively, at T (in units with $\hbar \equiv k_B \equiv 1$) = 300.
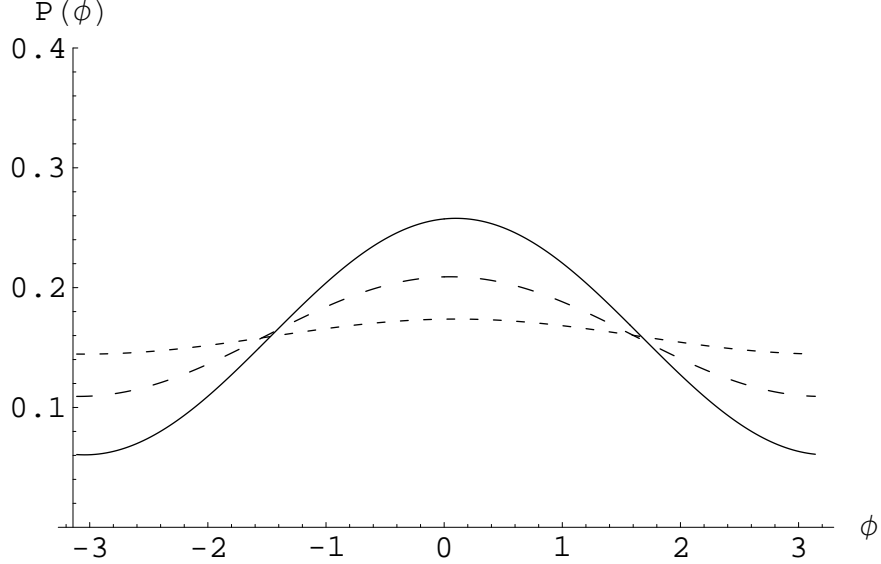

FIG. 8: Quantum phase distribution, $\mathcal{P}(\phi)$ given by Eq. (73), at the north pole of the phase space for a two-level atom initially in an atomic squeezed state, as a function of ϕ (in radians), for different environmental conditions. The system squeezing parameter (64) Θ has been taken as = - 0.5494, the bath squeezing parameter $r = 1$, and $\gamma_0 = 0.025$. The continuous curve corresponds to a temperature $T = 0$ and an evolution time $t = 0.1$, while the small-dashed and large-dashed curves correspond to evolution times $t = 0.1$ and 0.05, respectively, at T (in units with $\hbar \equiv k_B \equiv 1$) = 300.

A_p is defined by Eqs. (63) and (67), and is usually fixed by normalization as in the above equations, where $|A_p|^2 = (\cosh \Theta)^{-1}$ which is equal to 1 for $\Theta = 0$ [56], implying an infinite initial squeezing ζ of the system (64). The expression in Eq. (72) for the south pole in the phase space and that in Eq. (73) for the north pole in the phase space differ from each other by a sign in the second part of the expressions. The contrast between them can be seen clearly from Figs. 7 and 8. As seen from the figures, with the increase in temperature T or the exposure time to the environment t, the phase distribution curves flatten out indicating increased phase diffusion. These curves bring out another notable feature, viz., with the increase in bath exposure time t or temperature T, the effect of squeezing, indicated by the parameter r, is washed out. This behavior is analogous to the effect of squeezing in oscillator systems, where with the increase in bath exposure time t and temperature T, the non-stationary effects

introduced by the squeezed bath are washed out [60].

Eqs. (72) and (73) are easily seen to be normalized to unity. As in subsection IVB above, the effect of the environment shows up in the above equations only in the function $\gamma(t)$, responsible for decoherence. As was the case in the previous subsection IVB, from the forms of the function $\gamma(t)$, for an Ohmic bath, given by Eqs. (13) and (14) for $T = 0$ and for high T, respectively, we find that the second term on the right-hand side of Eqs. (72) and (73) has a power-law decay at zero T and an exponential decay at high T, and eventually the phase distribution tends to the uniform limit of $\frac{1}{2\pi}$ seen in the case in IVA. Thus the effect of the environment stays for a longer time at zero T as compared to high T, and eventually the distribution tends to the same uniform value irrespective of the initial state being a coherent or a squeezed state. As pointed out in [42, 45, 57], the state $|\zeta, p\rangle$ in (63) has an inherent squeezing which is represented by ζ in (64) and the environmental squeezing r is encapsulated in the function $\gamma(t)$ given by (10). Thus the results (72) and (73) bring out the relative importance of the different squeezing sources and hence are applicable in the context of the experiment of Kuzmich *et al.* [23] concerning the role of the environment on the atomic quantum nondemolition measurements and squeezing.

V. CONCLUSIONS

In this paper we have analyzed the quantum phase distribution of a number of physically interesting systems interacting with their environment via a QND type of coupling. We have taken our system to be either an oscillator (harmonic or anharmonic) or a two-level atom (or equivalently, a spin-1/2 system), and modeled the environment as a bath of harmonic oscillators, initially in a general squeezed thermal state, from which the common thermal bath results may be easily extracted by setting the squeezing parameters to zero. We have explicitly evaluated the phase distribution and worked out the effects of different environmental parameters on the dynamics of the system starting with various initial states.

In particular, for a harmonic oscillator system in QND interaction with its environment (Section IIIA), we have considered two different initial conditions of the system, starting (1) in a coherent state, and (2) in a squeezed coherent state. The phase distribution corresponding to the unitary evolution in the second case is more tilted than that in the first case, which is a signature of the squeezing inherent in the initial state of the system. We have next taken an anharmonic oscillator (Section IIIB), which could arise, for example, from the interaction of a single mode of the quantized electromagnetic field with a Kerr medium, and constructed its phase distribution, again for different initial conditions: (1) the system starting in a Kerr state, and (2) the system starting in a squeezed Kerr state. With an increase in the evolution time t, indicating an increase in exposure to the environment, the quantum phase distribution in the first case shifts as well as diffuses.

We have then studied the phase distribution for a discrete two-level atom (Section IV), for different initial conditions of the system, starting (1) in a Wigner-Dicke state, which is the atomic analogue of the standard Fock state, (2) in an atomic coherent state, which is the atomic analogue of the Glauber coherent state, and (3) in an atomic squeezed state. In the first test case, the phase distribution is uniform and is independent of any bath dynamics. In the other two cases, it is seen that the effect of the environment stays for a longer time at zero temperature than that at high temperature, and eventually the distribution tends to the uniform value of the first case, irrespective of the initial state of the system.

In all the cases considered, a broadening of the phase distribution curve, indicating an increase in phase diffusion, results with an increase in the bath temperature T or bath squeezing parameter r or evolution time t. The broadening of the curves, of course, preserves the normalization of the phase distribution. Even though each system considered is an 'open' system, we could make use of the underlying group symmetries of the system Hamiltonians, because of the QND nature of the system-environment coupling. Our quantitative results are of potential use in the analysis of a broad class of relevant experimental situations dealing with quantum nondemolition measurements and squeezing.

Acknowledgments

[1] W. H. Louisell, *Quantum Statistical Properties of Radiation* (John Wiley and Sons, 1973).

[2] A. O. Caldeira and A. J. Leggett, Physica A **121**, 587 (1983).
[3] W. H. Zurek, Phys. Today **44**, 36 (1991); Prog. Theor. Phys. **87**, 281 (1993).
[4] V. Hakim and V. Ambegaokar, Phys. Rev. A **32**, 423 (1985).
[5] C. M. Smith and A. O. Caldeira, Phys. Rev. A **36**, 3509 (1987); *ibid* **41**, 3103 (1990).
[6] H. Grabert, P. Schramm and G. L. Ingold, Phys. Rep. **168**, 115 (1988).
[7] S. Banerjee and R. Ghosh, Phys. Rev. A **62**, 042105 (2000).
[8] S. Banerjee and R. Ghosh, Phys. Rev. E **67**, 056120 (2003).
[9] J. Shao, M-L. Ge and H. Cheng, Phys. Rev. E **53**, 1243 (1996).
[10] D. Mozyrsky and V. Privman, Journal of Stat. Phys. **91**, 787 (1998).
[11] G. Gangopadhyay, M. S. Kumar and S. Dattagupta, J. Phys. A: Math. Gen. **34**, 5485 (2001).
[12] V. B. Braginsky, Y. I. Vorontsov and K. S. Thorne, Science **209**, 547 (1980).
[13] V. B. Braginsky and F. Ya. Khalili, in *Quantum Measurements*, edited by K. S. Thorne (Cambridge University Press, Cambridge, 1992).
[14] V. B. Braginsky and Yu. I. Vorontsov, Usp. Fiz. Nauk **114**, 41 (1974) [Sov. Phys. Usp. **17**, 644 (1975)]; V. B. Braginsky, Yu. I. Vorontsov, and V. D. Krivchenkov, Zh. Eksp. Teor. Fiz. **68**, 55 (1975) [Sov. Phys. JETP **41**, 28 (1975)].
[15] V. B. Braginsky, Yu. I. Vorontsov and F. Ya. Khalili, Pis'ma Zh. Eksp. Teor. Fiz. **27**, 296 (1978) [Sov. Phys. JETP Lett.. **27**, 276 (1978)].
[16] W. G. Unruh, Phys. Rev. D **19**, 2888 (1979).
[17] J. N. Hollenhorst, Phys. Rev. D **19**, 1669 (1979).
[18] C. M. Caves, K. S. Thorne, R. W. P. Drever, V. D. Sandberg, and M. Zimmerman, Rev. Mod. Phys. **52**, 341 (1980).
[19] D. F. Walls and G. J. Milburn, *Quantum Optics* (Springer, Berlin, 1994).
[20] W. H. Zurek, in *The Wave-Particle Dualism*, edited by S. Diner, D. Fargue, G. Lochak and F. Selleri (D. Reidel Publishing Company, Dordrecht, 1984).
[21] M. F. Bocko and R. Onofrio, Rev. Mod. Phys. **68**, 755 (1996).
[22] R. Onofrio and L. Viola, Phys. Rev. A **58**, 69 (1998).
[23] A. Kuzmich, N. P. Bigelow and L. Mandel, Europhys. Lett. **42**, 481 (1998).
[24] J. Clausen, J. Salo, V. M. Akulin and S. Stenholm, Phys. Rev. A **72**, 062104 (2005).
[25] S. Banerjee and R. Ghosh, J. Phys. A: Math. Theo. **40**, 1273 (2007).
[26] Q. A. Turchette, C. J. Myatt, B. E. King, C. A. Sackett, D. Kielpinski, W. M. Itano, C. Monroe and D. J. Wineland, Phys. Rev. A **62**, 053807 (2000).
[27] V. Perinova, A. Luks and J. Perina, *Phase in Optics* (World Scientific, Singapore, 1998).
[28] P. A. M. Dirac, Proc. R. Soc. Lond. A **114**, 243 (1927).
[29] L. Susskind and J. Glogower, Physics **1**, 49 (1964).
[30] P. Carruthers and M. M. Nieto, Rev. Mod. Phys. **40**, 411 (1968).
[31] D. T. Pegg and S. M. Barnett, J. Mod. Opt. **36**, 7 (1989); Phys. Rev. A **39**, 1665 (1989).
[32] J. H. Shapiro, S. R. Shepard and N. C. Wong, Phys. Rev. Lett. **62**, 2377 (1989).
[33] J. H. Shapiro and S. R. Shepard, Phys. Rev. A **43**, 3795 (1991).
[34] M. J. W. Hall, Quantum Opt. **3**, 7 (1991).
[35] G. S. Agarwal, S. Chaturvedi, K. Tara and V. Srinivasan, Phys. Rev. A **45**, 4904 (1992).
[36] S. Banerjee and R. Ghosh, eprint quant-ph/0703054.
[37] C. C. Gerry and R. Grobe, Phys. Rev. A **49**, 2033 (1994).
[38] V. Buzek, Phys. Rev. A **39**, 5432 (1989).
[39] W. G. Unruh, Phys. Rev. A **51**, 992 (1995).
[40] G. M. Palma, K-A. Suominen and A. K. Ekert, Proc. R. Soc. Lond. A **452**, 567 (1996).
[41] D. P. DiVincenzo, Phys. Rev. A **51**, 1015 (1995).
[42] G. S. Agarwal and R. P. Singh, Phys. Lett. A **217**, 215 (1996).
[43] R. H. Dicke, Phys. Rev. **93**, 99 (1954).
[44] F. T. Arecchi, E. Courtens, R. Gilmore and H. Thomas, Phys. Rev. A **6**, 2211 (1972).
[45] J. P. Dowling, G. S. Agarwal and W. P. Schleich, Phys. Rev. A **49**, 4101 (1994).
[46] C. M. Caves and B. L. Schumaker, Phys. Rev. A **31**, 3068 (1985); B. L. Schumaker and C. M. Caves, Phys. Rev. A **31**, 3093 (1985).
[47] M. O. Scully and M. S. Zubairy, *Quantum Optics* (Cambridge University Press, Cambridge, 1997).
[48] M. Kitagawa and Y. Yamamoto, Phys. Rev. A **34**, 3974 (1986).
[49] V. Bargmann, Ann. Math. **48**, 568 (1947).
[50] K. Wodkiewicz and J. H. Eberly, J. Opt. Soc. Am. B **2**, 458 (1985).
[51] C. C. Gerry, Phys. Rev. A **35**, 2146 (1987).
[52] C. C. Gerry and A. Benmoussa, Phys. Rev. A **62**, 033812 (2000); H. Ui, Progress of Theoretical Physics **44**, 703 (1970).
[53] M. V. Satyanarayana, Phys. Rev. D **32**, 400 (1985); P. Marian, Phys. Rev. A **44**, 3325 (1991).
[54] A. Erdelyi, W. Magnus, F. Oberhettinger and F. G. Tricomi, *Higher Transcendental Functions*, Vol. I (McGraw-Hill, New York, 1953).
[55] J. M. Radcliffe, J. Phys. A: Gen. Phys. **4**, 313 (1971).
[56] M. A. Rashid, J. Math. Phys. **19**, 1391 (1978).
[57] G. S. Agarwal and R. R. Puri, Phys. Rev. A **41**, 3782 (1990).
[58] C. Aragone, E. Chalbaud and S. Salamo, J. Math. Phys. **17**, 1963 (1976).

[59] D. A. Varshalovich, A. N. Moskalev and V. K. Khersonskii, *Quantum Theory of Angular Momentum* (World Scientific, Singapore, 1988).
[60] S. Banerjee and J. Kupsch, J. Phys. A: Math. Gen. **38**, 5237 (2005).